

# Conductivity and magnetoresistance of $\text{La}_{0.7}\text{Ce}_{0.3}\text{MnO}_3$ thin films under photoexcitation

A Thiessen<sup>1</sup>, E Beyreuther<sup>1</sup>, R Werner<sup>2</sup>, R Kleiner<sup>2</sup>, D Koelle<sup>2</sup> and L M Eng<sup>1</sup>

<sup>1</sup>Institut für Angewandte Photophysik, Technische Universität Dresden, D-01062 Dresden, Germany

<sup>2</sup>Physikalisches Institut and Center for Collective Quantum Phenomena in LISA<sup>+</sup>, Universität Tübingen, Auf der Morgenstelle 14, D-72076 Tübingen, Germany

E-mail: andreas.thiessen@iapp.de, elke.beyreuther@iapp.de

**Abstract.**  $\text{La}_{0.7}\text{Ce}_{0.3}\text{MnO}_3$  thin films of different thicknesses, degrees of  $\text{CeO}_2$ -phase segregation and oxygen deficiency, grown on  $\text{SrTiO}_3$  single crystal substrates, were comparatively investigated with respect to both their spectral and temperature-dependent photoconductivity (PC) and their magnetoresistance (MR) behaviour under photoexcitation. While as-grown films were insensitive to optical excitation, oxygen reduction appeared to be an effective way to decrease the film resistance, but the film thickness was found to play a minor role. However, from the evaluation of the spectral behaviour of the PC and the comparison of the MR of the LCeMO/substrate-samples with a bare substrate under illumination we find that the photoconductivity data reflects not only contributions from (i) photogenerated charge carriers in the film and (ii) carriers injected from the photoconductive substrate (as concluded from earlier works), but also (iii) a decisive parallel photoconduction in the  $\text{SrTiO}_3$  substrate. Furthermore – also by analyzing the MR characteristics – the unexpected occurrence of a strong electroresistive effect in the sample with the highest degree of  $\text{CeO}_2$  segregation and oxygen deficiency could be attributed to the electroresistance of the  $\text{SrTiO}_3$  substrate as well. The results suggest a critical reconsideration and possibly a reinterpretation of several previous photoconductivity and electroresistance investigations of manganite thin films on  $\text{SrTiO}_3$ .

PACS numbers: 71.30.h, 72.40.w, 73.50.Pz, 75.47.Lx

## 1. Introduction

Doped rare-earth manganites, also referred to as mixed-valence or colossal-magnetoresistive (CMR) manganites, have attracted a flurry of interest for decades [1, 2, 3, 4]. They are primarily of academic interest within the study of fundamental concepts in solid state physics addressing issues such as their multifaceted electronic/magnetic phase diagrams, their strong coupling between lattice, charge, spin, or orbital degrees of freedom, their sensitivity towards external fields, the high spin polarization in some compounds, or the occurrence of electronic phase separation in chemically homogeneous samples. While the technological value of bulk crystals seems to be limited, e.g. due to the low magnetic Curie temperatures, thin films of selected compositions have the potential to play a role within tunable heterostructures in future all-oxide/all-perovskite electronic devices.

The present work focuses on two of the younger aspects of manganite-compound research: the possibility of tetravalent-ion substitution in order to achieve effective electron-doping, e.g. for fabricating all-manganite diodes, and the behaviour under external optical excitation.

For the last two decades, *tetravalent-ion substituted* rare-earth manganites (with  $\text{La}_{1-x}\text{Ce}_x\text{MnO}_3$  being the most prominent among them) have been discussed intensively as a potential electron-doped counterpart to the well-known divalent-ion substituted and thus hole-doped manganites. A summary of the debate, focusing on possible (thin film) preparation routes and the proof of an effective electron-doping, i.e., a mixed  $\text{Mn}^{2+/3+}$  valence, has been given in previous works [5, 6]. For instance, as a number of investigations have shown, as-prepared  $\text{La}_{0.7}\text{Ce}_{0.3}\text{MnO}_3$  (LCeMO) films do not show their nominal Mn valence of +2.7 but are in fact hole-doped due to oxygen excess. On the other hand, post-deposition oxygen reduction decreases the Mn valence towards the nominal value but also leads to a pronounced resistance increase and the loss of the manganite-typical metal-insulator transition (MIT). Interestingly, a decisive conductivity increase and the recovery of the MIT can be induced by *photoexcitation* [7]. However, the exact origin of these effects remained hidden to date. In very recent x-ray photoemission measurements, exploring the Mn valence as a function of oxygen content and illumination intensity in variably thick LCeMO films on  $\text{SrTiO}_3$ , evidence for the decisive role of photogenerated-charge injection from the substrate to the films was reported, but an additional manganite-intrinsic photoconductivity could not be completely excluded [8]. This is one of the starting points where the present work sets in.

Compared to the number of investigations reflecting on the tunability of the manganites' conductivity and other physical properties by doping, magnetic or strain fields, studies of *the effects of photonic excitations on manganites* are still a quite small research field. For a further discussion we define the photoresistance *PR* as follows:

$$PR := \frac{R_{\text{dark}} - R_{\text{illum}}}{R_{\text{illum}}} = \frac{R_{\text{dark}}}{R_{\text{illum}}} - 1, \quad (1)$$

with  $R_{dark}$  being the sample resistance in the dark, and  $R_{illum}$  being the resistance under light excitation. Thus a decrease of the resistance under illumination results in a *positive* PR, i.e., an appreciable *photoconductivity*.

A survey of the previous literature is given in [7, 9]. In short, after the first discovery of photoconductivity in a mixed-valence manganite, namely in a Pr<sub>0.7</sub>Ca<sub>0.3</sub>MnO<sub>3</sub> single crystal [10], a number of single-crystalline as well as thin-film manganite compounds were studied under various photoexcitation conditions, and a plenty of effects were reported. A general coherent microscopic picture of the photoresponse is still lacking to date. Roughly, the effects belong to one of the four following groups:

- photonic excitation of electrons from the valence to the conduction band [11, 12],
- photoinduced demagnetization [13, 14],
- disturbance of charge and orbital order in insulating charge ordered manganites by photoelectrons [15, 16, 17, 18], and
- injection of photogenerated charge carriers from the substrate into the thin-film channel [7, 9, 19, 20].

The last of these four mechanisms naturally occurs in thin films only; but there it plays a major and possibly technologically interesting role. In La<sub>0.7</sub>Sr<sub>0.3</sub>MnO<sub>3</sub> films on SrTiO<sub>3</sub>, which were illuminated with a broad-band white-light source and exhibited a *negative* PR, Katsu et al. concluded an injection of optically generated electrons from the SrTiO<sub>3</sub> substrate into the hole-doped film followed by the recombination of both carrier types within the film leading to a resistance increase [19, 20]. In our two previous works, where we observed *positive* PR in La<sub>0.7</sub>Ce<sub>0.3</sub>MnO<sub>3- $\delta$</sub>  [7] and La<sub>0.7</sub>Ca<sub>0.3</sub>MnO<sub>3- $\delta$</sub>  [9] films on SrTiO<sub>3</sub>, we gave a similar interpretation. By the comparative evaluation of the wavelength dependence of the PR and the surface photovoltage we had concluded that at least part of the photogenerated carriers must stem from interband transitions in the substrate or from carrier excitation from interface states, the latter explaining the PR below the SrTiO<sub>3</sub> band gap energy, and not solely from the manganite film. However, these investigations were limited to a single film with a thickness of 10 nm only.

Thus, the present experiments were planned and conducted purposely to clarify the microscopic scenario of the phototransport in Ce-doped manganite thin films employing a broader set of films.

Extended resistance-vs.-temperature ( $R$ - $T$ ) data of the films under different illumination conditions was acquired in order to systematically analyse the influence of film thickness, oxygen content, and degree of phase separation on (i) the dark transport, which is reported in a separate paper [21], and (ii) the phototransport, which is discussed in section 3.1.

Moreover, due to the well-known strong coupling of magnetic order and electronic transport in the manganites it appeared to be indispensable to study the magnetotransport under illumination for a further understanding of the microscopic nature of the observed photoconductivity. The corresponding magnetoresistance (MR) measurements and results for selected samples are presented in section 3.2.

Finally, the LCeMO film exhibiting the strongest disorder showed (apart from its photoconductivity) a rather unexpected electroresistive effect. There, magnetoresistance measurements were employed to understand this (side) effect as well.

## 2. Experimental

Three different LCeMO films were grown by pulsed laser deposition on SrTiO<sub>3</sub> (100) single crystal substrates. Details on growth and structural analysis can be found in reference [6]. Samples  $\ddagger$  B and C were grown under the same oxygen partial pressure of  $p(\text{O}_2)=0.25$  mbar but are different in thickness (30 nm vs. 100 nm), while samples C and D have the same thickness but D was grown under a decisively lower oxygen pressure, which led to microscopic segregation of CeO<sub>2</sub> clusters. Thus, the comparison of B and C provides information on the thickness dependence of the films' photoresponse, and contrasting C and D is supposed to give comparative insight to the PCs dependence on the degree of phase segregation.

To separate the influence of the oxygen stoichiometry from any of the above parameters, each sample was studied at three different states of oxygen reduction, which were prepared by heating in a low-pressure oxygen atmosphere (see table 1).

For reference measurements of the magnetoresistance, also a *bare* SrTiO<sub>3</sub> (100) single crystal was reduced by applying the same procedure as for preparing the *highly reduced* state of the thin-film samples.

The illumination setup consists of the monochromatized output of a Xe arc lamp, several collimating and focusing lenses, mirrors, and a control loop for adjusting the photon flux by moving a neutral density filter, mounted on a motorized translation stage. Details can be found in [7, 22].

The photoconductivity measurements were carried out in an optical liquid-nitrogen cryostat (Optistat DN by Oxford Instruments). The illuminated area on the sample was around 20 mm<sup>2</sup>. The magnetotransport measurements were performed in an optical liquid-helium cryostat with a superconducting magnet (Microstat MO by Oxford Instruments) producing a magnetic field  $B$  perpendicular to the sample surface. Here, a sample area of 8 mm<sup>2</sup> was illuminated. All resistance measurements were carried out in two-point geometry using an electrometer (Keithley 6517B), applying a measuring voltage of 1 V, unless stated otherwise. Contacts were made with conducting silver paste, placed 3 mm apart.

$\ddagger$  Note that sample labelling begins with B and not with A in order to keep the sample names of our previous works [7, 8].

**Table 1.** Overview of the heating parameters for the preparation of differently oxygen-reduced LCeMO/SrTiO<sub>3</sub> samples. Note that each of the states was prepared for each of the three samples B, C, D. The *as-prepared* state means that the sample has not been furtherly treated after the PLD growth.

state	T (°C)	p(O <sub>2</sub> ) (mbar)	t (h)
as-grown	—	—	—
slightly reduced	480	10 <sup>-6</sup>	1
highly reduced	700	10 <sup>-8</sup>	2

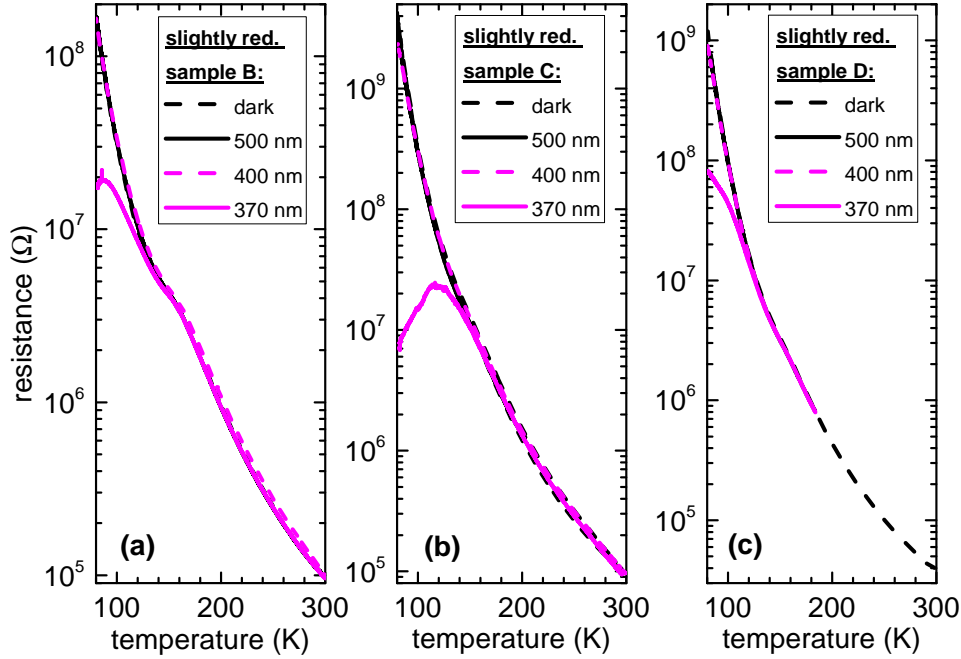


**Figure 1.** (a)-(c): *Slightly reduced* LCeMO films B, C, and D: Temperature dependence of the resistance in the dark and under illumination with three different wavelengths. The light intensities were 810  $\mu\text{W}/\text{mm}^2$  at 370 nm, 750  $\mu\text{W}/\text{mm}^2$  at 400 nm, and 600  $\mu\text{W}/\text{mm}^2$  at 500 nm.

### 3. Results and Discussion

#### 3.1. Photoconductivity

As a first result, *no change* of the  $R$ - $T$  characteristics under illumination could be observed in the three *as-prepared* films. This is in accordance with our former XPS study [8], where the same samples showed no change of the Mn valence under additional photoexcitation in the visible and near-UV range, as well.

At second, let us consider the photoresponse of the *slightly reduced* samples. Figure 1 depicts the  $R$ - $T$  curves in the dark and under illumination at three different wavelengths, i.e., 370 nm (above the SrTiO<sub>3</sub> bandgap  $E_g = 3.2 \text{ eV} \simeq 387 \text{ nm}$ ), 400 nm (slightly below  $E_g$ ), and 500 nm (substantially below  $E_g$ ). There is no resistance change under illumination at room temperature. A significant photoinduced decrease of the resistance is observed below 150 K and only for the 370-nm illumination. For sample C the MIT appears to be recovered. Figure 2(a) contains the spectral photoresistance (PR) data at 80 K. Here, a noticeable increase of the PR is observable below 385...390 nm (corresponding to  $E_g$ ) for all three samples.

Proceeding with the discussion of the *highly reduced* LCeMO films, as expected, the dark resistances are substantially higher than in the slightly reduced samples, see figure 3. At a measuring voltage of 1 V, all samples exhibit an insulating behaviour in the whole investigated temperature range and no clear MIT. Similarly to the slightly reduced films, illumination leads to a significant decrease of the resistance at low temperatures, but makes no effect at 300 K. Different to the case of the slightly reduced films [cf. figure 2(a)] which exhibit moderate PR values up to 120 %, the PR at 80 K shows dramatically high values already for longer wavelengths, see figure 2(b). Below 395 nm (B, C) and 385 nm (D) the PR increases even more strongly with decreasing wavelength. Remarkably, the PR of the thinner (30 nm) film B is higher than the PR of the thicker (100 nm) film C. Assuming an intrinsic charge carrier generation in the film, one would expect the opposite to happen, since the thicker film must absorb more light and thus exhibit the larger PR. If charge carrier injection from the substrate is the dominating process, the thinner film should, as indeed observed here, have the higher PR, since it passes more photons to the substrate. Thus, at a first glance, the current observation points towards the charge injection scenario postulated before in ref. [7]. On the other hand, regarding the case of the slightly reduced films, the PR of the thinner film B is *lower* than the PR of the thicker films C and D [see fig. 2(a), again]. It is

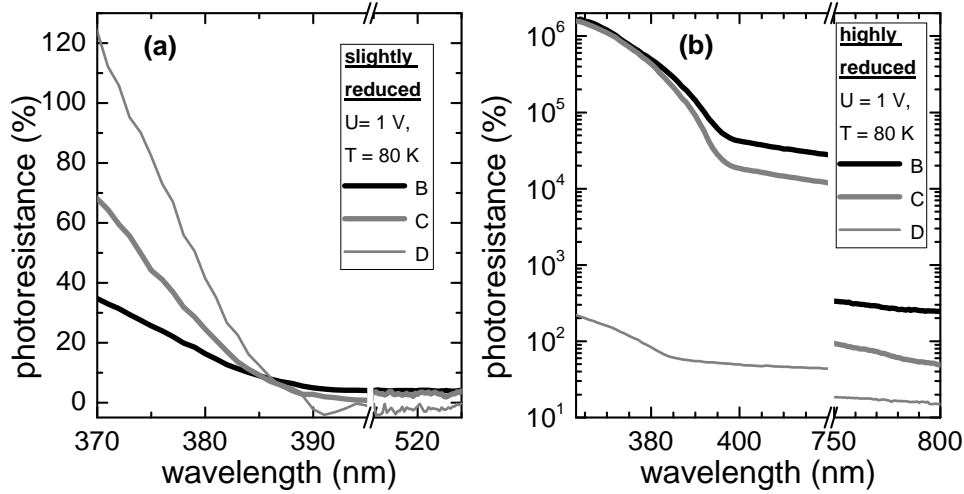


**Figure 2.** Photoresistance of (a) the *slightly reduced* and (b) the *highly reduced* LCeMO films at 80 K, recorded with a constant photon flux of  $6.8 \mu\text{W}/\text{mm}^2$  at 370 nm. Note that the data was recorded with a photon flux around two orders of magnitude lower than in the measurements of figs. 1 and 3, since here the monochromator exit slit was reduced to 1 mm width (instead of 10 mm) in order to achieve a higher energy resolution and thus a sharper photoresistance spectrum.

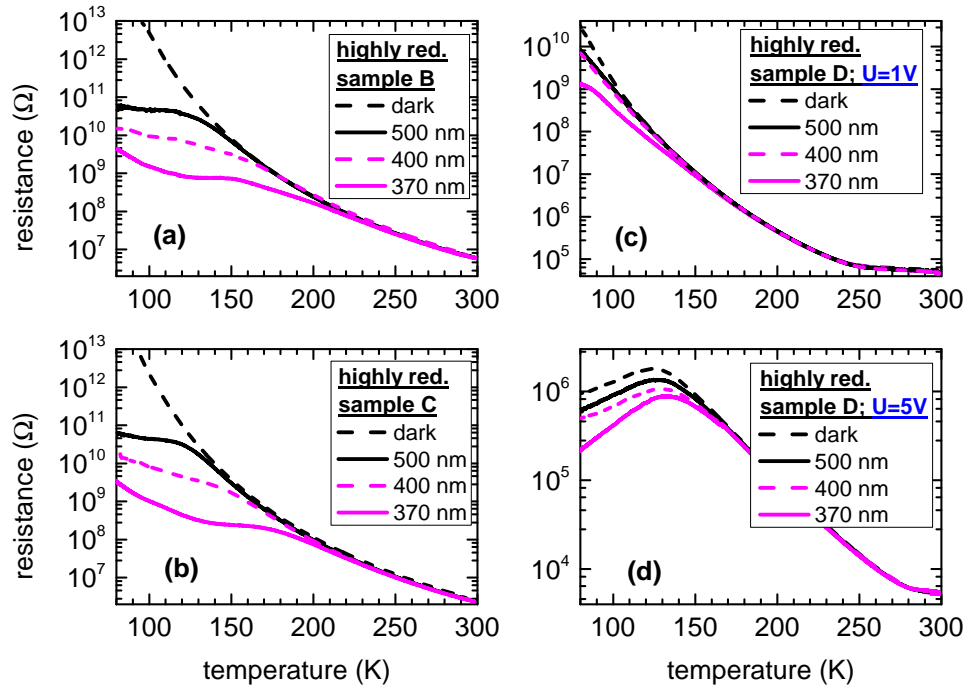


**Figure 3.** *Highly reduced* LCeMO films:  $R$ - $T$  characteristics in the dark and under illumination (at the same light intensities as in figure 1). (a), (b) Samples B and C at 1 V measurement voltage. (c), (d) Sample D at 1 V and 5 V measurement voltage.

conceivable, that both processes, intrinsic carrier generation in the LCeMO and injection of photogenerated carrier from the substrate coexist, but with different weight depending on the degree of oxygen reduction.

Interestingly, the resistance of film D strongly depends on the measuring voltage. As visible in figure 3(d), the resistance at 5 V is at least one order of magnitude lower than at 1 V [figure 3(c)] over the whole temperature range investigated here. Furthermore, at 5 V, an MIT appears at 135 K, whose transition temperature rises under illumination. Indeed, as shown in figure 4, the current-voltage characteristics of the highly reduced sample D is highly nonlinear and asymmetric at 300 K as well as at 80 K, which points towards an enhanced inhomogeneity of the film. We note that the corresponding I-V curves of samples B and C (not shown here) exhibit a linear shape at 300 K and nonlinear asymmetric shapes at 80 K, but the latter with very low currents in the pA range, which limits their significance.

### 3.2. Magnetoresistance

Due to the well-known strong interplay between charge transport and magnetic order in the mixed-valence manganites, we performed systematic measurements of the magnetoresistance as a function of magnetic field and temperature in order to achieve a profound understanding of the effect of illumination and measuring voltage on the charge transport in the

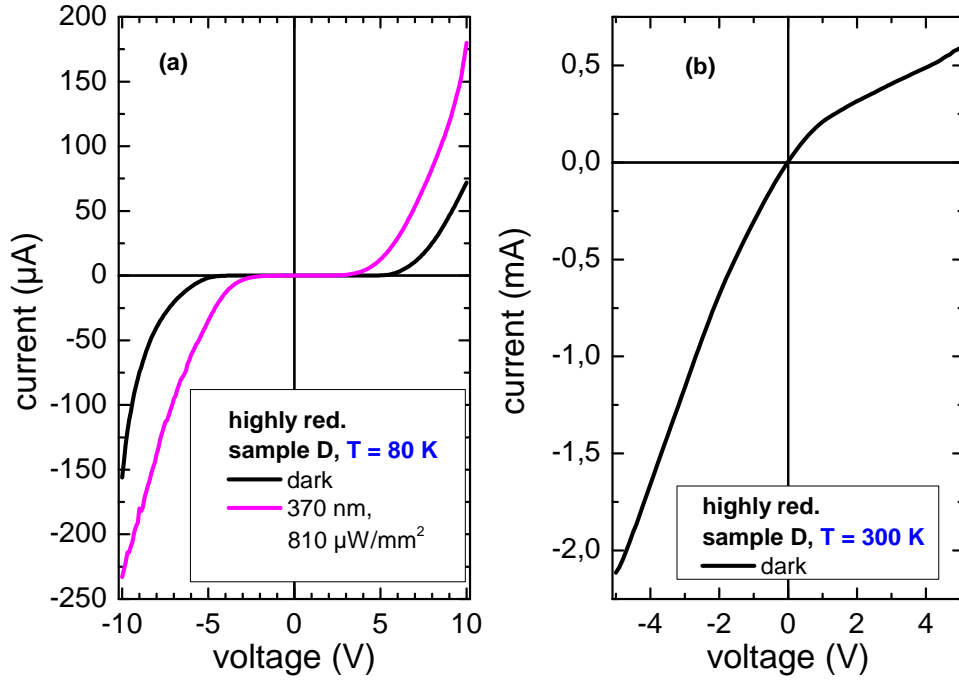


**Figure 4.** Current-voltage characteristics of the highly reduced sample D at 80 K (a) and at 300 K (b).

*highly reduced* LCeMO samples. Thus, an extended temperature range between 5 K and 300 K was studied using a liquid-helium cryostat for the following selected samples:

- The *highly reduced sample C* was measured in order to clarify the origin of the photoconductivity and the photoinduced MIT.
- The *highly reduced sample D* was studied in order to clarify the origin of the electrical-field-induced MIT. Since the interpretation of those results turned out to be complex and the electroresistance is more a side effect within the present study, we have exported the information and discussion for this sample into the supplement.
- The *as-prepared sample C* and a *reduced bare SrTiO<sub>3</sub>* single crystal were chosen for reference measurements.

Prior to presenting our experimental findings, we briefly recall the necessary background needed to evaluate the MR data:

In the literature on the CMR effect, the following definition of the *MR* is frequently used:

$$MR = \frac{R(B) - R(0)}{R(0)} = \frac{R(B)}{R(0)} - 1 \quad . \quad (2)$$

In mixed-valent manganites, the resistance at zero field  $R(0)$  is larger than the resistance in an external magnetic field  $R(B)$  (negative MR). Then the above definition gives values between -1 and 0.

A quantitative model describing the field dependence of the MR is given by Wagner et al. [23]. Here, the following proportionalities are obtained:

$$MR(B) \propto \mathcal{B}_J^2[g\mu_B JB/(k_B T)] \quad \text{for } T > T_C \quad , \quad (3)$$

and

$$MR(B) \propto \mathcal{B}_J[g\mu_B JB/(k_B T)] \quad \text{for } T < T_C \quad , \quad (4)$$

with  $\mathcal{B}_J$  being the Brillouin function,  $J$  the total angular momentum of the magnetic moments at the starting and the ending position of a hopping process, and  $g$  the gyromagnetic factor with  $g = 2$ . Furthermore, from geometrical considerations the following relation to calculate the radii of magnetic clusters  $r_{MC}$  in the paramagnetic phase (which were also interpreted as magnetic polarons [24]) can be derived:

$$r_{MC} = \left( \frac{3}{4\pi} \frac{J}{J(Mn^{3+})} \right)^{1/3} \cdot c \quad , \quad (5)$$

with  $J(Mn^{3+}) = 2$  (valid for the  $Mn^{3+}$  ion without magnetic interactions) and  $c$  being the lattice constant. In this model, the ratio  $J/J(Mn^{3+})$  is an estimate of the number of magnetically coupled Mn ions.

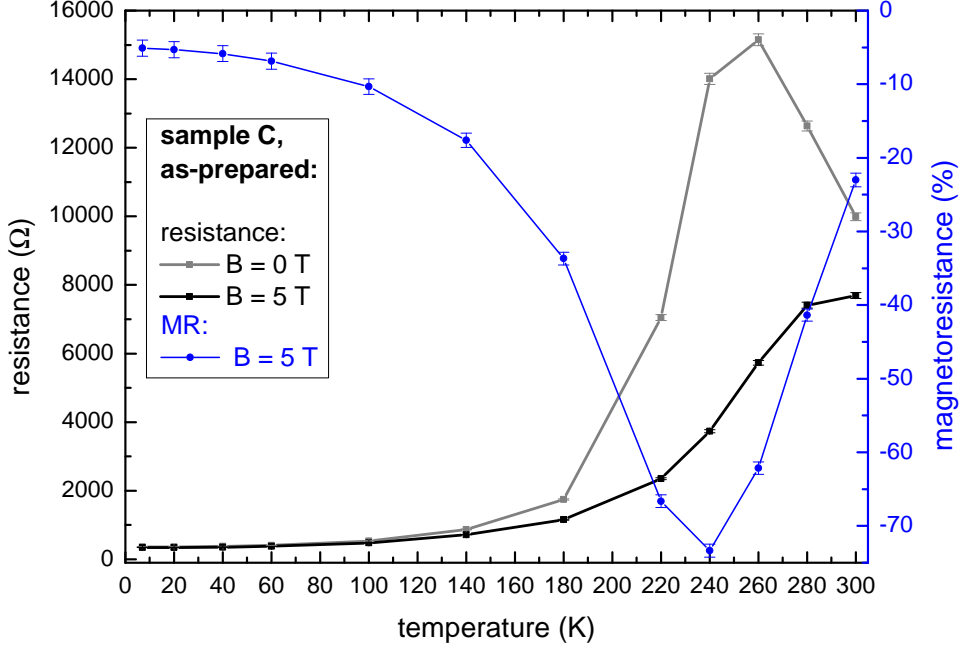


**Figure 5.** Resistance and magnetoresistance of the *as-prepared* sample C.

**3.2.1. As-prepared sample C** As a first reference, the magnetoresistance of sample C in the non-reduced state was studied – only in the dark, since all non-reduced samples did not show any photoconductivity. In a magnetic field of 5 T the resistance is clearly reduced and the MIT shifts from 250 K to 300 K (see fig. 5). This means a negative magnetoresistance over the whole temperature range from 5 to 300 K, with an extremum of -73% around the MIT. For some selected temperatures, the magnetic-field dependence of the MR [fig. 6(a)] is evaluated by fitting the data with the Brillouin function  $\mathcal{B}_J(g\mu_B JB/k_B T)$ , see eqs. (3), (4).

As expected from theory, the MR above the MIT temperature is proportional to  $\mathcal{B}^2$  while approaching a linear dependence ( $\propto \mathcal{B}$ ) below the MIT.  $J$  is a free parameter within the regression analysis and represents the total angular momentum of the magnetic polarons. From fig. 6(b), which displays  $J$  as a function of the temperature, we see that  $J$  has its maximum in the range of the MIT and decreases for both higher and lower temperatures. At 220 K the total angular momentum peaks with  $J = 192$ , which corresponds to 96 magnetically ordered Mn<sup>3+</sup> ions. Employing eq. (5), such a magnetic polaron has a radius of 1 nm, which is consistent with literature data for other hole-doped manganites [23, 25].

In the metallic phase, the dark resistance between 40...110 K is reproduced by  $\rho(T) = \rho_0 + \alpha T^{2.5}$  with  $\rho_0 = 3.65 \cdot 10^{-5} \Omega \text{m}$ , which is a typical behaviour for hole-doped manganites, too [26]. However, the value of  $\rho_0$  is comparatively high for an epitaxial film [27], which is attributed to a high defect density due to the nanoscopic CeO<sub>2</sub> phase segregation and the oxygen excess.

**3.2.2. Highly reduced sample C** The resistance in zero field and the magnetoresistance at 5 T of the highly reduced sample C in the dark as well as under 370-nm illumination are depicted in figs. 7(a) and (b), respectively.

As found before, *in the dark* the sample is insulating in the whole temperature range, while the resistance is beyond our detection limit below 80 K. The MR is negative and decreases with decreasing temperature down to -60% at 80 K. As shown in fig. 8(a), the MR vs. B data is reproduced by  $\mathcal{B}^2$  down to 140 K, with  $J$  growing from 20 to 50 with decreasing temperature, which corresponds to magnetic-polaron radii between 0.5 nm and 0.7 nm in accordance with the carrier localization lengths of 0.4...0.8 nm (as estimated in ref. [21]). Between 130 K and 110 K the MR can be fitted by a linear combination of  $\mathcal{B}^2$  and  $\mathcal{B}$  [fig. 8(b)], while  $\mathcal{B}$  reproduces the MR-vs.-T data below 100 K [fig. 8(b)]. A phase transition from the paramagnetic to the ferromagnetic state, starting at 130 K, exhibiting a coexistence of para- and ferromagnetic areas down to 110 K, and ending in a completely ferromagnetic state at 100 K, would be consistent with such a behaviour.

*Under illumination*, from 200 K towards lower temperatures, the resistance is dramatically lower than in the dark, showing a small saturation between 150 K and 80 K [fig. 7(a)]. At 80 K a strong decrease of the resistance is visible, while the shape of the R-vs.-T is not typical for a mixed-valence manganite having a MIT. The MR at 5 T is negative between 300 K and 110 K and decreases with falling temperature – as for the dark case. From 110 K towards lower temperatures the MR increases and, surprisingly, becomes positive below 70 K, which is non-typical for a manganite as well. The magnetic-field dependence of the MR can be approximated by  $\mathcal{B}^2$  with  $J = 50 \dots 20$  between 300 K and 130 K [fig. 9(a)], as for the dark case. Also similar to the behaviour under dark conditions, at 110 K a linear combination of  $\mathcal{B}^2$  and  $\mathcal{B}$  is suitable, while at 90 K  $\mathcal{B}$  gives the best fit [fig. 9(b)]. However, as a main result, which will be discussed in

§ For convenience, we shortly write  $\mathcal{B}$  instead of  $\mathcal{B}_J(g\mu_B JB/k_B T)$  in the following.



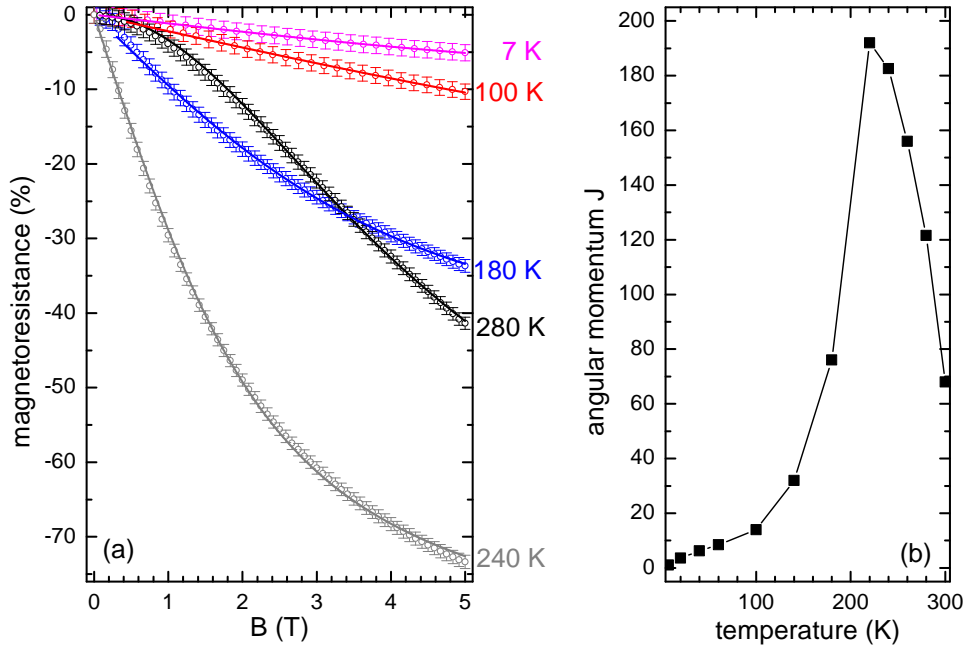


**Figure 6.** As-prepared sample C: (a) Magnetic-field dependence of the MR for selected temperatures with the corresponding Brillouin-function fits; (b) angular momentum  $J$ , as derived from the fitting procedures.

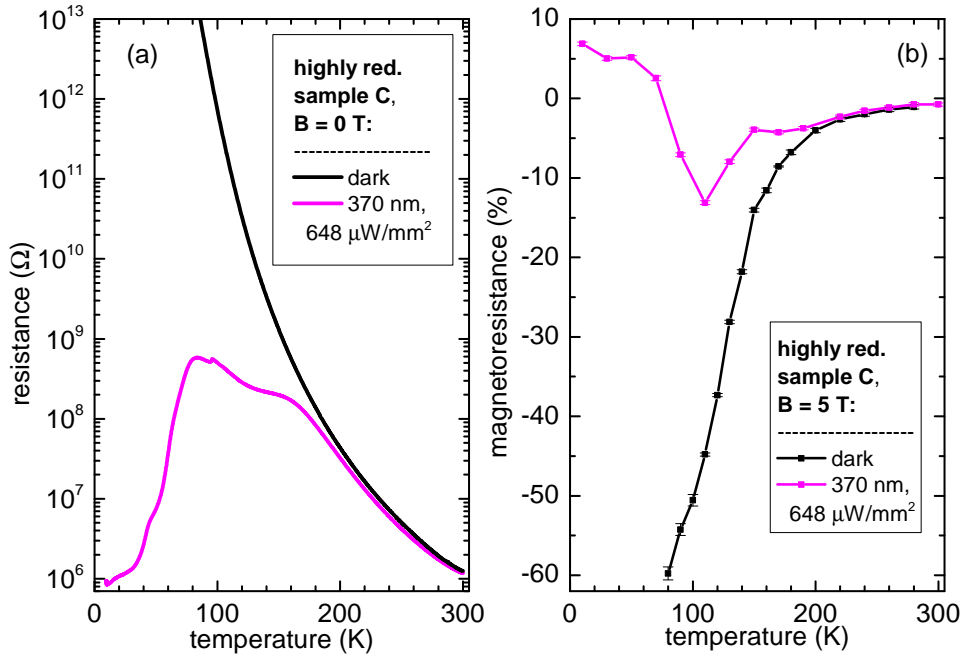


**Figure 7.** Photoconductivity of the *highly reduced* sample C: (a) Resistance vs. temperature in zero field in the dark and under 370-nm illumination; (b) magnetoresistance in the dark and under illumination.

detail in sec. 3.2.4, the occurrence of a positive MR is in conflict with a scenario that postulates the MIT to stem from the injection of photogenerated carriers from the substrate into the LCeMO film.

**3.2.3. Reduced bare SrTiO<sub>3</sub>** As visible in fig. 10, the dark resistance of the reduced SrTiO<sub>3</sub> can be reliably measured only in the limited range between 300 K and 250 K. Obviously, the annealing procedure could not increase the electron concentration enough to allow transport measurements. Tests with higher voltages up to 100 V gave similar results. Illumination with 370 nm at 648  $\mu\text{W}/\text{mm}^2$  causes a dramatic decrease of the resistance of at least five orders of magnitude. We find a maximum of the resistance at 270 K and a subsequent slight decrease at lower temperatures, followed by a steeper decrease below 70 K [fig. 7(a)]. Qualitatively, the curve shape is equivalent to the respective  $R$ - $T$  curve of the highly reduced and illuminated sample C for  $T < 70$  K. Furthermore, in this low-temperature range, the bare-SrTiO<sub>3</sub> resistance is at least one order of magnitude smaller than the resistance of sample C. Thus, we conclude that the MIT of the highly reduced sample C is not primarily LCeMO-intrinsic but has its origin in the parallel conduction in the

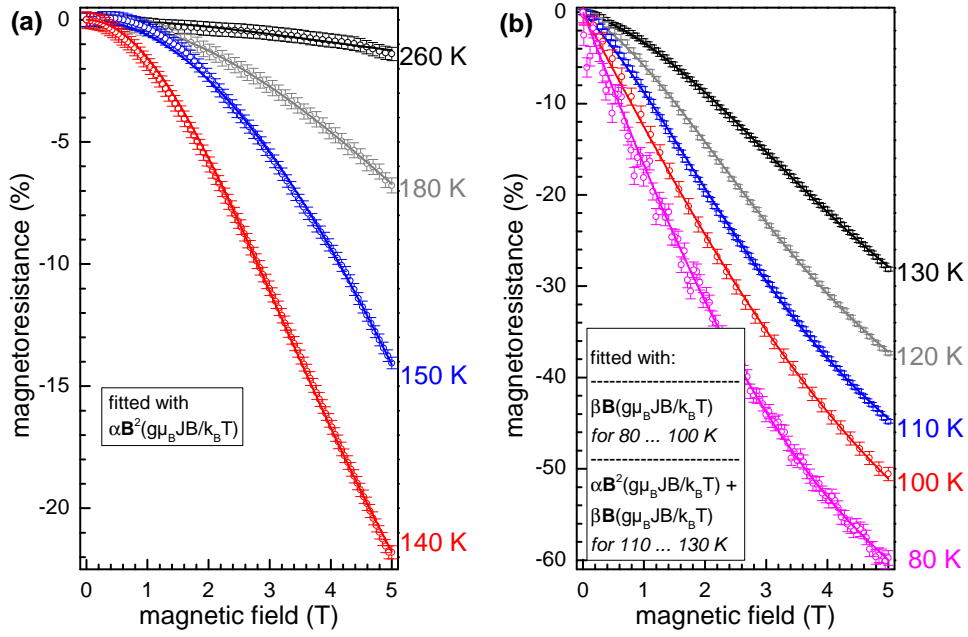


**Figure 8.** Highly reduced sample C in the dark: MR-vs.-magnetic-field data for selected temperatures, fitted with  $B^2$  for higher temperatures (a) and with  $B$  or a linear combination of  $B^2$  and  $B$  for lower temperatures (b).

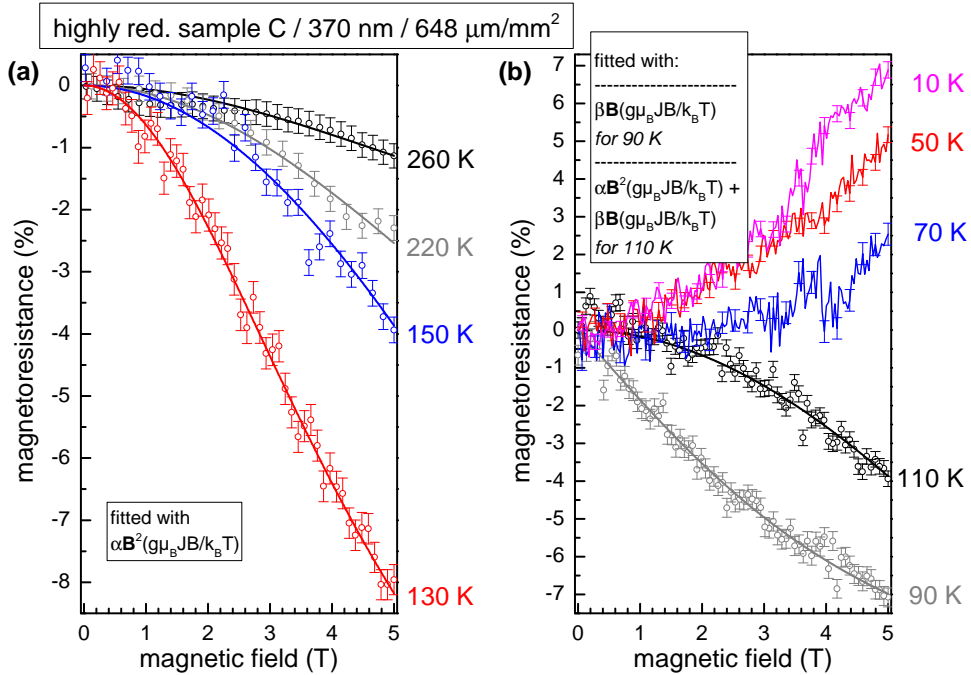


**Figure 9.** Highly reduced sample C under 370-nm illumination: MR-vs.-magnetic-field data for selected temperatures with corresponding Brillouin-function fits down to 90 K. For the three lowest temperatures of 10, 50, and 70 K positive MR is observed.

photoconductive SrTiO<sub>3</sub> substrate.

The MR of the bare SrTiO<sub>3</sub> reference was only studied under illumination due to the very high dark resistance. Two data sets with electrical contacts at two different locations on the sample surface were recorded, see fig. 11(a) for the temperature dependence of the MR at 5 T and fig. 11(b) for the magnetic-field dependence of the MR. The resistances at low temperatures differ noticeably for the two sample locations, which points towards an inhomogeneous oxygen diffusion during annealing. Below 60 K a positive MR of 5% is observed, at decisively lower temperatures (down to 7 K) values as large as 147% are reached. The MR(B) dependence is approximately linear, which was already reported in the literature [28, 29] for highly reduced SrTiO<sub>3</sub>.

**3.2.4. Discussion of the magnetoresistance results** Here, we consider the implications of the MR results on our understanding of the photoconductivity results, while the implications on the interpretation of the electroresistive effect of sample D have been exported to the supplement.



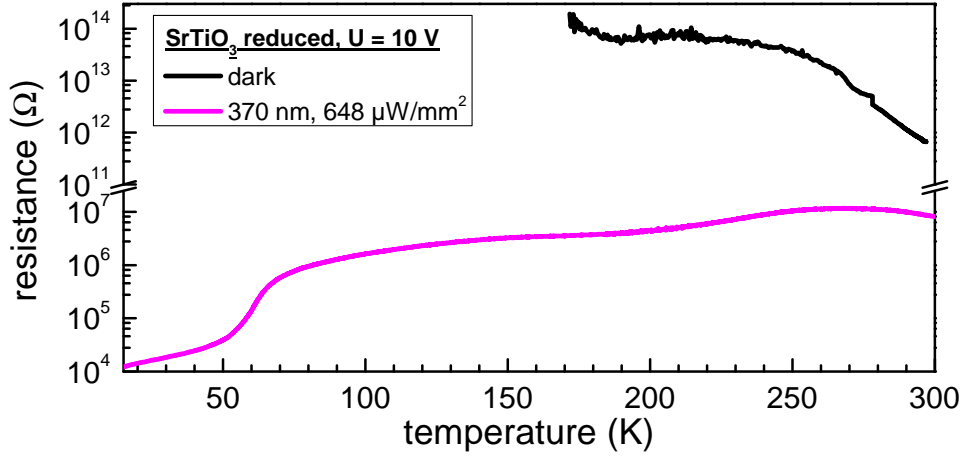


**Figure 10.** Resistance vs. temperature characteristics of the bare SrTiO<sub>3</sub> reference crystal. Note the break of the resistance axis.

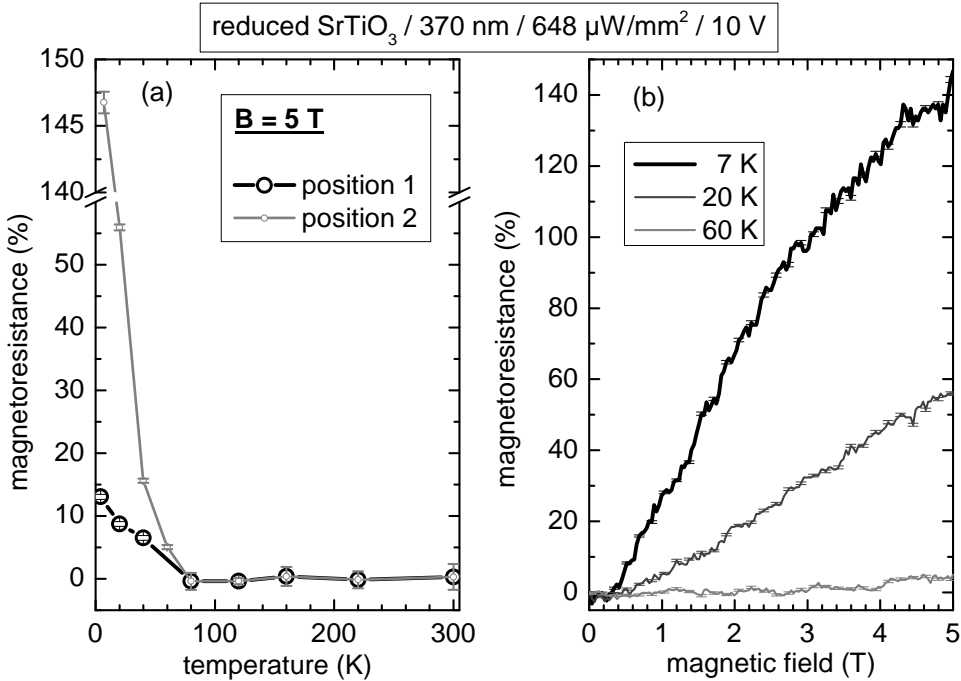


**Figure 11.** Bare SrTiO<sub>3</sub> sample: (a) Temperature dependence of the MR in a magnetic field of 5 T, measured at two different sample surface positions; (b) corresponding magnetic-field dependence of the MR at selected temperatures (position 2).

Regarding the reference MR measurements on the bare reduced SrTiO<sub>3</sub> single crystal, both the light-induced MIT at 80 K and the positive MR below 70 K in the highly reduced sample C clearly reflect the occurrence of parallel charge transport within the SrTiO<sub>3</sub> substrate. However, the plateau in the  $R$ - $T$  curves of the highly reduced samples B and C under 370-nm illumination might still be interpreted as an intrinsic effect from the manganite films, i.e., the electron concentration is increased by photogenerated-charge injection from the substrate and/or by photogenerated carriers from the film itself, but not strong enough to cause a complete delocalization of the carriers [30]. Thus, the photoconductivity above 80 K is in agreement with the XPS results of ref. [8]. However, one discrepancy between the former XPS work and the present results remains: In the latter, no photoconductivity at room temperature was observed, while in the first, there is a clear change of the Mn valence when illuminating at 300 K. One possible explanation hints towards photoinduced electron generation confined to the sample surface, for which the XPS is sensitive. The effect might be too small to decisively change the electron concentration in the whole film, which is the reason, why the present transport measurements cannot detect this effect. Finally, from all methods used here and previously (resistance measurements, XPS, magnetoresistance – all in the dark and under illumination), one can summarize that none of the contributions, which were discussed to contribute to the observed photoconductivity, i. e., (i) intrinsic carrier generation in the LCeMO films, (ii) injection of carriers from the photoconductive SrTiO<sub>3</sub> substrate into the film, and (iii) parallel (photo-)conduction in the SrTiO<sub>3</sub>, can be totally excluded. All three effects may coexist, however with different weights depending on the temperature and the illumination parameters.

#### 4. Summary and conclusions

Differently thick La<sub>0.7</sub>Ce<sub>0.3</sub>MnO<sub>3</sub> films on SrTiO<sub>3</sub> with a variable degree of oxygen content and CeO<sub>2</sub> phase segregation were studied with respect to its conductivity and magnetoresistance under illumination, in order to achieve a deeper understanding of the photoconductivity and the light-induced metal-insulator transition.

While formerly the coexistence of (i) photogenerated carriers within the the LCeMO films and (ii) carriers injected from the substrate or from interface states was proposed to be the origin for the  $R$ - $T$  characteristics under illumination, the observation of *positive* magnetoresistance under illumination for both the LCeMO/SrTiO<sub>3</sub> heterostructures and a bare SrTiO<sub>3</sub> single crystal strongly points towards a third (coexisting) mechanism influencing the measured resistance behaviour: parallel photoconduction in the substrate.

Unexpectedly, the highly reduced LCeMO film with the strongest CeO<sub>2</sub> phase segregation showed an electrical-field induced MIT, which could, however, after the evaluation of the magnetoresistance behaviour, be ascribed to the charge transport in the SrTiO<sub>3</sub> substrate, too.

Finally, we conclude that the role of the SrTiO<sub>3</sub> substrate in previous studies of the photoinduced properties of manganite thin films, e.g., refs. [7, 9, 11, 12], has to be questioned critically. In the future, it might be more reasonable to perform investigations of the intrinsic photoconductivity of manganites on either films grown on less photoresponsive substrates than SrTiO<sub>3</sub> (e.g., LaAlO<sub>3</sub>) or on bulk crystals.

#### Acknowledgement

This work was kindly supported by the German Science Foundation (DFG, grant no. BE 3804/2-1).

#### References

- [1] A.P. Ramirez. Colossal magnetoresistance. *J. Phys.: Condens. Matter*, 9(39):8171–8199, 1997. doi:10.1088/0953-8984/9/39/005.
- [2] J. M. D. Coey, M. Viret, and S. von Molnár. Mixed-valence manganites. *Adv. Phys.*, 48(2):167–293, 1999. doi:10.1080/000187399243455.
- [3] A.-M. Haghir-Gosnet and J.-P. Renard. CMR manganites: physics, thin films and devices. *J. Phys. D: Appl. Phys.*, 36(8):R127–R150, 2003. doi:10.1088/0022-3727/36/8/201.
- [4] K. Dörr. Ferromagnetic manganites: spin-polarized conduction versus competing interactions. *J. Phys. D: Appl. Phys.*, 39:R125–R150, 2006. doi:10.1088/0022-3727/39/7/R01.
- [5] E. Beyreuther, S. Grafström, L. M. Eng, C. Thiele, and K. Dörr. XPS investigation of Mn valence in lanthanum manganite thin films under variation of oxygen content. *Phys. Rev. B*, 73:155425, 2006. doi:10.1103/PhysRevB.73.155425.
- [6] R. Werner, C. Raisch, V. Leca, V. Ion, S. Bals, G. Van Tendeloo, T. Chassé, R. Kleiner, and D. Koelle. Transport, Magnetic, and Structural Properties of La<sub>0.7</sub>Ce<sub>0.3</sub>MnO<sub>3</sub> Thin Films: Evidence for Hole-Doping. *Phys. Rev. B*, 79:054416, 2009. doi:10.1103/PhysRevB.79.054416.
- [7] E. Beyreuther, A. Thiessen, S. Grafström, L. M. Eng, M. C. Dekker, and K. Dörr. Large photoconductivity and light-induced recovery of the insulator-metal transition in ultrathin La<sub>0.7</sub>Ce<sub>0.3</sub>MnO<sub>3-δ</sub> films. *Phys. Rev. B*, 80:075106, 2009. doi:10.1103/PhysRevB.80.075106.
- [8] A. Thiessen, E. Beyreuther, S. Grafström, K. Dörr, R. Werner, R. Kleiner, D. Koelle, and L. M. Eng. The Mn<sup>2+</sup>/Mn<sup>3+</sup> state of La<sub>0.7</sub>Ce<sub>0.3</sub>MnO<sub>3</sub> by oxygen reduction and photodoping. *J. Phys.: Condens. Matter*, 26:045502, 2014. doi:10.1088/0953-8984/26/4/045502.
- [9] E. Beyreuther, A. Thiessen, S. Grafström, K. Dörr, and L. M. Eng. Large photoconductivity of oxygen-deficient La<sub>0.7</sub>Ca<sub>0.3</sub>MnO<sub>3</sub>/SrTiO<sub>3</sub> heterostructures. *J. Phys.: Condens. Matter*, 22:175506, 2010. doi:10.1088/0953-8984/22/17/175506.
- [10] V. Kiryukhin, D. Casa, J. P. Hill, B. Keimer, A. Vigiliante, Y. Tomioka, and Y. Tokura. An X-ray-induced insulator-metal transition in a magnetoresistive manganite. *Nature*, 386:813–815, 1997. doi:10.1038/386813a0.
- [11] A. Gilibert, R. Cauro, M. G. Medici, J. C. Grenet, H. S. Wang, Y. F. Hu, and Q. Li. Photoconductivity in manganites. *J. Supercond.*, 13:285–290, 2000. doi:10.1023/A:1007760202272.
- [12] R. Cauro, A. Gilibert, J. P. Contour, R. Lyonnet, M. G. Medici, J. C. Grenet, C. Leighton, and I. K. Schuller. Persistent and transient photoconductivity in oxygen-deficient La<sub>2/3</sub>Sr<sub>1/3</sub>MnO<sub>3-δ</sub> thin films. *Phys. Rev. B*, 63:174423, 2001. doi:10.1103/PhysRevB.63.174423.
- [13] M. Matsubara, Y. Okimoto, T. Ogasawara, S. Iwai, Y. Tomioka, H. Okamoto, and Y. Tokura. Photoinduced switching between charge and orbital ordered insulator and ferromagnetic metal in perovskite manganites. *Phys. Rev. B*, 77:094410, 2008. doi:10.1103/PhysRevB.77.094410.
- [14] G. M. Gao, C. L. Chen, L. A. Han, and X. S. Cao. Photoinduced resistivity change of electron-doped La<sub>0.8</sub>Te<sub>0.2</sub>MnO<sub>3</sub> film. *J. Appl. Phys.*, 105:033707, 2009. doi:10.1063/1.3077183.
- [15] M. Fiebig, K. Miyano, Y. Tomioka, and Y. Tokura. Visualization of the Local Insulator-Metal Transition in Pr<sub>0.7</sub>Ca<sub>0.3</sub>MnO<sub>3</sub>. *Science*, 280:1925–1928, 1998. doi:10.1126/science.280.5371.1925.
- [16] M. Fiebig, K. Miyano, Y. Tomioka, and Y. Tokura. Reflection spectroscopy on the photoinduced local metallic phase of Pr<sub>0.7</sub>Ca<sub>0.3</sub>MnO<sub>3</sub>. *Appl. Phys. Lett.*, 74(16):2310–2312, 1999. doi:10.1063/1.123834.
- [17] I. I. Smolyaninov, V. N. Smolyaninova, C. C. Davis, B.-G. Kim, S.-W. Cheong, and R. L. Greene. High Resolution Study of Permanent Photoinduced Reflectivity Changes and Charge-Order Domain Switching in Bi<sub>0.3</sub>Ca<sub>0.7</sub>MnO<sub>3</sub>. *Phys. Rev. Lett.*, 87(12):127204, 2001. doi:10.1103/PhysRevLett.87.127204.
- [18] S. Chaudhuri and R. C. Budhani. Complementarity of perturbations driving insulator-to-metal transition in a charge-ordered manganite. *EPL*, 81:17002, 2008. doi:10.1209/0295-5075/81/17002.
- [19] H. Katsu, H. Tanaka, and T. Kawai. Photocarrier injection effect on double exchange ferromagnetism in (La, Sr)MnO<sub>3</sub>/SrTiO<sub>3</sub> heterostructure. *Appl. Phys. Lett.*, 76:3245, 2000. doi:10.1063/1.126595.
- [20] H. Katsu, H. Tanaka, and T. Kawai. Dependence of carrier doping level on the photo control of (La,Sr)MnO<sub>3</sub>/SrTiO<sub>3</sub> functional heterojunction. *J. Appl. Phys.*, 90:4578–4582, 2001. doi:10.1063/1.1410328.
- [21] A. Thiessen, E. Beyreuther, R. Werner, R. Kleiner, D. Koelle, and L. M. Eng. Electrical-transport characteristics of as-grown and oxygen-reduced La<sub>0.7</sub>Ce<sub>0.3</sub>MnO<sub>3</sub> films: calculation of hopping energies, Mn valences, and carrier localization lengths. 2014. URL: <http://arxiv.org/abs/1408.4569>.
- [22] E. Beyreuther, A. Thiessen, J. Becherer, S. Grafström, K. Dörr, and L. M. Eng. Probing electronic defect states in manganite/SrTiO<sub>3</sub> heterostructures by surface photovoltage spectroscopy. *Mat. Sci. Engin. B*, 176(5):446–452, 2011. doi:10.1016/j.mseb.2010.12.014.

- [23] P. Wagner, I. Gordon, L. Trappeniers, J. Vanacken, F. Herlach, V. V. Moshchalkov, and Y. Bruynseraede. Spin Dependent Hopping and Colossal Negative Magnetoresistance in Epitaxial Nd<sub>0.52</sub>Sr<sub>0.48</sub>MnO<sub>3</sub> Films in Fields up to 50 T. *Phys. Rev. Lett.*, 81:3980, 1998. doi:[10.1103/PhysRevLett.81.3980](https://doi.org/10.1103/PhysRevLett.81.3980).
- [24] J. M. D. Coey, M. Viret, L. Ranno, and K. Ounadjela. Electron Localization in Mixed-Valence Manganites. *Phys. Rev. Lett.*, 75:3910–3913, 1995. doi:[10.1103/PhysRevLett.75.3910](https://doi.org/10.1103/PhysRevLett.75.3910).
- [25] J. M. De Teresa, M. R. Ibarra, P. A. Algarabel, C. Ritter, C. Marquina, J. Blasco, J. Garcia, A. del Moral, and Z. Arnold. Evidence for magnetic polarons in the magnetoresistive perovskites. *Nature*, 386:256, 1997. doi:[10.1038/386256a0](https://doi.org/10.1038/386256a0).
- [26] J. M. De Teresa, M. R. Ibarra, J. Blasco, J. Garcia, C. Marquina, P. A. Algarabel, Z. Arnold, K. Kamenev, C. Ritter, and R. von Helmolt. Spontaneous behavior and magnetic field and pressure effects on La<sub>2/3</sub>Ca<sub>1/3</sub>MnO<sub>3</sub> perovskite. *Phys. Rev. B*, 54:1187, 1996. doi:[10.1103/PhysRevB.54.1187](https://doi.org/10.1103/PhysRevB.54.1187).
- [27] A. Gupta, G. Q. Gong, Gang Xiao, P. R. Duncombe, P. Lecoeur, P. Trouilloud, Y. Y. Wang, V. P. Dravid, and J. Z. Sun. Grain-boundary effects on the magnetoresistance properties of perovskite manganite films. *Phys. Rev. B*, 54(22):R15629–R15632, 1996. doi:[10.1103/PhysRevB.54.R15629](https://doi.org/10.1103/PhysRevB.54.R15629).
- [28] O. N. Tufte and E. L. Stelzer. Magnetoresistance in semiconducting strontium titanate. *Phys. Rev.*, 173(3):775–777, September 1968. doi:[10.1103/PhysRev.173.775](https://doi.org/10.1103/PhysRev.173.775).
- [29] Z. Q. Liu, W. M. Lü, X. Wang, Z. Huang, A. Annadi, S. W. Zeng, T. Venkatesan, and Ariando. Magnetic-field induced resistivity minimum with in-plane linear magnetoresistance of the Fermi liquid in SrTiO<sub>3-x</sub> single crystals. *Phys. Rev. B*, 85:155114, 2012. doi:[10.1103/PhysRevB.85.155114](https://doi.org/10.1103/PhysRevB.85.155114).
- [30] A. Seeger, P. Lunkenheimer, J. Hemberger, A. A. Mukhin, V. Y. Ivanov, A. M. Balbashov, and A. Loidl. Charge carrier localization in La<sub>1-x</sub>Sr<sub>x</sub>MnO<sub>3</sub> investigated by ac conductivity measurements. *J. Phys.: Condens. Matter*, 11:3273, 1999. doi:[10.1088/0953-8984/11/16/009](https://doi.org/10.1088/0953-8984/11/16/009).